Supporting Information

Photochemical Barcodes

Sicheng Tang,§ Yang Zhang,§ Pravat Dhakal,§ Laura Ravelo,
Cheyenne L. Anderson, Kevin M. Collins and Françisco M. Raymo*

Laboratory for Molecular Photonics, Departments of Biology and Chemistry, University of Miami,

1301 Memorial Drive, Coral Gables, FL 33146-0431

E-Mail: fraymo@miami.edu

---

§ Contributed equally

* Corresponding author

Experimental Procedures

Materials and Methods. Chemicals were purchased from commercial sources and used as received. CH_2Cl_2 and MeCN were distilled over CaH_2. H_2O (18.2 MΩ cm) was purified with a Barnstead International NANOpure DIamond Analytical system. Compounds **5** and **6** were prepared following literature protocols.[S1,S2] Electrospray ionization mass spectrometry (EISMS) was performed with a Bruker micrOTO-Q II spectrometer. Nuclear magnetic resonance (NMR) spectra were recorded with a Bruker Avance 400 spectrometer. Absorption spectra were recorded with a Varian Cary 100 Bio spectrometer in quartz cells with a path length of 1.0 cm. Emission spectra were recorded with a Varian Cary Eclipse spectrometer in aerated solutions. Fluorescence quantum yields were determined against EtOH solutions of either the acetate salt of Cresyl Violet (ϕ_F = 0.54) or the perchlorate salt of Oxazine 1 (ϕ_F = 0.15), following a literature protocol.[S3] Photolyses were performed in aerated solutions with a Luzchem Research LZC-4V photoreactor, operating at 350 nm (4.2 mW cm^{-2}). High-performance liquid chromatography (HPLC) was performed with an Agilent Microsorb 100-5 BDS column (4.6 × 250 mm) operated with a Shimadzu Nexera X2 system in MeCN/H_2O (9:1, v/v) at a flow rate of 1.0 mL min^{-1} and detection wavelength of 275 nm. Doped polymer films were prepared by spin coating CH_2Cl_2 solutions of poly(methyl methacrylate) (PMMA, 120 kDa, 20 mg mL^{-1}) and **1** (50 μg mL^{-1}) with a Chemat Technologies KW-4A spin coater at 1,200 rpm for 60 s on glass coverslips. Doped polymer beads were prepared by pouring dropwise aliquots (1.0 mL) of tetrahydrofuran (THF) solutions of polyturene (PS, 44 kDa, 1.0 mg mL^{-1}) and **1**, **2** or **3** (50 μg mL^{-1}) into H_2O/EtOH (6:1, v/v, 5.0 mL). The resulting dispersions were maintained at ambient temperature for 3 hours in an open vial and used directly for the photolysis and spectroscopic experiments. Aliquots (10 μL) of the dispersions were transferred on glass coverslips, dried in an oven at 120 °C for 2 min and imaged. Fluorescence images were recorded with a Leica SP5 confocal laser-scanning microscope.

Chemical Synthesis of 1 and 2. A solution of **3** (200 mg, 0.32 mmol) and **6** (298 mg, 1.3 mmol) in MeCN (30 mL) was heated under reflux for 12 hours. The solvent was distilled off under reduced pressure and the residue was purified by column chromatography [SiO_2, hexanes/AcOEt (95:5 → 90:10, v/v)] to give **1** (30 mg, 10%) as a pink solid and **2** (20 mg, 8%) as a purple solid. **1**: ESIMS: *m/z* = 923.3530 $[M + H]^+$ (*m/z* calcd. for $C_{54}H_{46}BF_2N_6O_6$ = 923.3540); ^1H NMR (CD3Cl): δ = 7.75 (1H, d, 8 Hz), 7.64 (1H, d, 8 Hz), 7.44 (2H, d, 16 Hz), 7.37–7.29 (5H, m), 7.26–7.23 (1H, m), 7.21–7.07 (6H, m), 6.90 (2H, t, 7 Hz), 6.82–6.73 (4H, m), 6.69 (2H, d, 8 Hz), 6.64–6.56 (2H, m), 5.14 (2H, d, 19 Hz), 4.84 (2H, d, 19 Hz), 2.46 (3H, s), 1.64 (6H, s), 1.26 (6H, s); ^{13}C NMR [$(CD_3)_2CO$]: δ = 154.73, 152.94, 147.30, 146.84, 140.77, 137.90, 135.96, 132.51, 131.04, 130.32, 129.13, 127.78, 127.41, 123.85, 123.76, 122.31, 120.64, 117.71, 117.52, 116.89, 108.76, 101.48, 101.35, 50.49, 39.87, 34.67, 31.58, 29.06, 26.37, 25.28, 22.64, 21.40, 20.69, 18.77, 14.10, 11.41. **2**: ESIMS: *m/z* = 772.3288 $[M + H]^+$ (m/z calcd. for $C_{47}H_{41}BF_2N_5O_3$ = 772.3271); ^1H NMR (CD_3CN): δ = 8.14 (1H, d, 16 Hz), 7.69 (2H, dd, 1 and 8 Hz), 7.50 (4H, t, 7 Hz), 7.46–7.36 (6H, m), 7.32 (1H, dd, 1 and 7 Hz), 7.28 (1H, dd, 1 and 8 Hz), 7.25–7.21 (2H, m), 7.12 (1H, td, 1 and 8 Hz), 7.08 (1H, d, 5 Hz), 6.97 (2H, t, 5 Hz), 6.89 (1H, td, 1 and 8 Hz), 6.80 (1H, d, 8 Hz), 5.10 (1H, d, 19 Hz), 4.87 (1H, d, 19 Hz), 2.47 (3H, s), 1.62 (3H, s), 1.50 (6H, d, 3 Hz), 1.25 (3H, s).

Chemical Synthesis of 3. A solution of **5** (500 mg, 1.7 mmol), 2,3,3-trimethyl-3*H*-indole (1.08 mg, 6.8 mmol) and trifluoroacetic acid (TFA, 50 μL, 0.7 mmol) in EtOH (30 mL) was heated under reflux for 12 hours. After cooling down to ambient temperature, the solvent was distilled off under reduced pressure. The residue was dissolved in AcOEt (50 mL) and washed with aqueous HCl (1 M, 3 × 50 mL). The organic layer was dried over Na_2SO_4 and the solvent was distilled off under reduced pressure. The residue was dissolved in CH_2Cl_2 (30 mL) and the resulting solution was degassed with Ar. 2,3-Dichloro-5,6-dicyano-1,4-benzoquinone (DDQ, 454 mg, 2.0 mmol) was added and the solution was stirred at ambient temperature under Ar for 30 min. After the sequential addition of Et_3N (3 mL, 21.5 mmol) and $BF_3{\cdot}Et_2O$ (3 mL, 23.4 mmol), the mixture was stirred for a further 3 hours under the same conditions and washed with a saturated aqueous solution of $NaHCO_3$ (3 × 30 mL). The organic layer was dried over Na_2SO_4 and the solvent was distilled off under reduced pressure. The residue was purified by column chromatography [SiO_2, hexanes/AcOEt (95:5 → 70:30, v/v)] to give **3** (120 mg, 11%) as a dark green solid. ESIMS: *m/z* = 621.3021 $[M + H]^+$ (*m/z* calcd. for $C_{40}H_{36}BF_2N_4$ = 621.3001); ^1H NMR

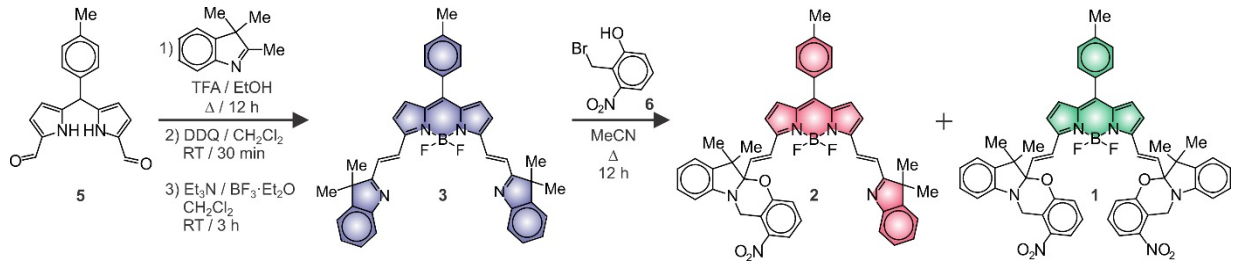

Figure S1. Synthesis of **1–3**.

[$(CD_3)_2CO$]: δ = 8.41 (2H, d, 16 Hz), 7.67–7.58 (6H, m), 7.53–7.47 (3H, m), 7.46 (3H, d, 5 Hz), 7.42–7.37 (2H, m), 7.31 (2H, t, 7 Hz), 7.07 (2H, d, 4 Hz), 2.50 (3H, s), 1.53 (12H, s); ^{13}C NMR [$(CD_3)_2CO$]: δ = 182.37, 154.43, 153.68, 147.23, 140.96, 137.30, 130.96, 130.68, 130.58, 129.29, 127.88, 127.48, 126.95, 126.37, 121.43, 121.20, 118.35, 52.66, 48.44, 39.30, 22.66, 20.58.

Photochemical Synthesis of 2 and 3. A solution of **1** (10 μM) in MeCN was maintained in the chamber of a photoreactor at 25 °C and irradiated at 350 nm (4.2 mW cm^{-2}) for 30 min. The reaction mixture was purified by HPLC [Agilent Microsorb 100-5 BDS (4.6 × 250 mm), MeCN/H_2O (9:1, v/v), 1.0 mL min^{-1}] to give **2** (5%) and **3** (14%).

Photokinetic Studies. Two consecutive photochemical reactions (Figure 1) are responsible for the conversion of **1** into **2** and **3**. The change in the molar concentration of **2** ([**2**]) with the irradiation time (*t*) is related to the quantum yields for the first (ϕ_{A1}) and second (ϕ_{A2}) photochemical steps as well as to the numbers of photons per unit area and time absorbed by **1** (I_1) and **2** (I_2) at λ_{Ac} (350 nm), according to equation (1).[S4]

$$\frac{d\,[\mathbf{2}]}{d\,t} = \phi_{\mathbf{A1}}\ I_{\mathbf{1}} - \phi_{\mathbf{A2}}\ I_{\mathbf{2}} \qquad (1)$$

At sufficiently low concentrations (<10 μM), the absorbance at λ_{Ac} is smaller than 0.1 and does not change significantly with the photochemical conversion. Under these conditions, I_1 and I_2 can be related to the number of incident photons (I_0) per unit area and unit time, the molar absorption coefficients of **1** (ε_1) and **2** (ε_2) at λ_{Ac}, the molar concentration of **1** ([**1**]), [**2**] and the length (*d*) of the optical path with equations (2) and (3) respectively.[S5] Additionally, any inner filter effects associated with the possible co-absorption of the photoproducts at λ_{Ac} become negligible.[S5]

$$I_{\mathbf{1}} = I_0\ \varepsilon_{\mathbf{1}}\ [\mathbf{1}]\ d \qquad (2)$$

$$I_{\mathbf{2}} = I_0\ \varepsilon_{\mathbf{2}}\ [\mathbf{2}]\ d \qquad (3)$$

Equations (1), (2) and (3) can be combined and integrated to give equation (4), where $[\mathbf{1}]_0$ is the initial molar concentration of **1**.[S6]

$$[\mathbf{2}] = \frac{[\mathbf{1}]_0\ \phi_{\mathbf{A1}}\ I_0\ \varepsilon_{\mathbf{1}}\ d}{\phi_{\mathbf{A2}}\ I_0\ \varepsilon_{\mathbf{2}}\ d - \phi_{\mathbf{A1}}\ I_0\ \varepsilon_{\mathbf{1}}\ d}\ \left[e^{-(\phi_{\mathbf{A1}}\ I_0\ \varepsilon_{\mathbf{1}}\ d)t} - e^{-(\phi_{\mathbf{A2}}\ I_0\ \varepsilon_{\mathbf{2}}\ d)t}\right] \qquad (4)$$

HPLC traces (Figure S2), collected during the photolytic transformation, provided estimates of [**2**] at increasing *t* (***a*** in Figure S3). I_0 was determined with a potassium ferrioxalate actinometer, according to an established procedure.[S7] ε_1 and ε_2 were estimated from the corresponding absorption spectra (Figures S4 and S5) and *d* was unitary. Fitting (***b*** in Figure S3) equation (4) to the plot of [**2**] against *t* indicated the values of ϕ_{A1} and ϕ_{A2} to be 0.001 and 0.003 respectively (Table S1). The coefficient of determination (C.O.D.) for the fitting was 0.99.

Nematode Imaging. *Caenorhabditis* (*C.) elegans* KG1180 *lite-1(ce314)* strain[S8] was grown at 20 °C on standard nematode growth medium (NGM) plates seeded with *Escherichia coli* OP50 bacteria and used for imaging experiments, as described previously.[S9S11] A dispersion of PS beads (0.02 mg mL^{-1}), doped with **1** (5% w/w), in sterile phosphate buffer saline (100 μL) was deposited dropwise on a standard seeded NGM plate. Age-matched adult hermaphrodites (~24 hours past the L4 larval stage) were transferred onto the plate and incubated at 20 °C for 2–5 hours to allow the bead uptake. Nematodes were transferred into a drop (~3 μL) of a H_2O solution of muscimol (10 mM) deposited on a 3% agarose pad prepared on a glass slide. After paralysis, the worms were covered with a coverslip, transferred on the stage of a confocal laser-scanning microscope and imaged. Muscimol allowed the retention of the fluorescent beads in the gut lumen during long-term imaging. At the end of the experiment, the coverslip was removed and the worms were transferred back to seeded NGM plates to reverse the muscimol block and confirm animal viability.

S1 Madhu, S.; Rao, M.; Shaikh, M.; Ravikanth, M. *Inorg. Chem.* **2011**, *50*, 4392–4400.

S2 Zhang, Y.; Swaminathan, S.; Tang, S.; Garcia-Amorós, J.; Boulina, M.; Captain, B.; Baker, J. D.; Raymo, F. M. *J. Am. Chem. Soc.* **2015**, *137*, 4709–4719.

S3 Wurth, C.; Grabolle, M.; Pauli, J.; Spieles, M.; Resch-Genger, U. *Nat. Protocols* **2013**, *8*, 1535–1550.

S4 Mauser, H.; Gauglitz, G. *Photokinetics: Theoretical Fundamentals and Applications*; Elsevier: Amsterdam, 1998.

S5 Sharma, A.; Schulman, S. G. *Introduction to Fluorescence Spectroscopy*; Wiley-Interscience: New York, 1999.

S6 Connors, K. C. *Chemical Kinetics: the Study of Reaction Rates in Solution*; Wiley-VCH: New York, 1990.

S7 Scaiano, J. C. *Handbook of Organic Photochemistry*; CRC Press: Boca Raton, 1989.

S8 Edwards, S. L., Charlie, N. K., Milfort, M. C., Brown, B. S., Gravlin, C. N., Knecht, J. E.; Miller, K. G. *PLoS Biol.* **2008**, 6, 1715–1729.

S9 Thapaliya, E. R.; Zhang, Y.; Dhakal, P.; Brown, A. S.; Wilson, J. N.; Collins, K. M.; Raymo, F. M. *Bioconjugate Chem.* **2017**, *28*, 1519–1528.

S10 Collins, K. M.; Koelle, M. R. *J. Neurosci.* **2013**, *33*, 761–775.

S11 Kim, E.; Sun, L.; Gabel, C. V.; Fang-Yen, C. *PLOS ONE* **2013**, *8*, e53419.

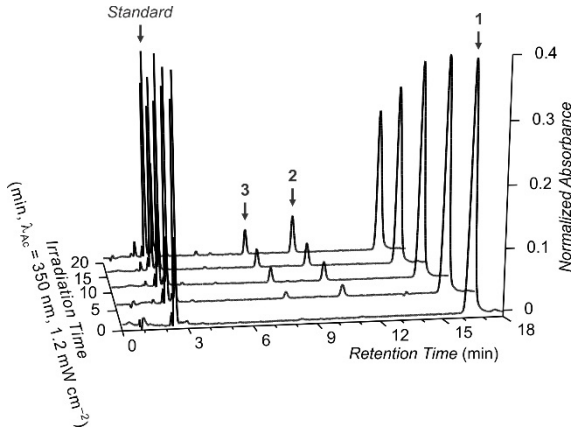

Figure S2. Chromatograms recorded before and after irradiation of a MeCN solution of **1** (10 μM) at 25 °C.

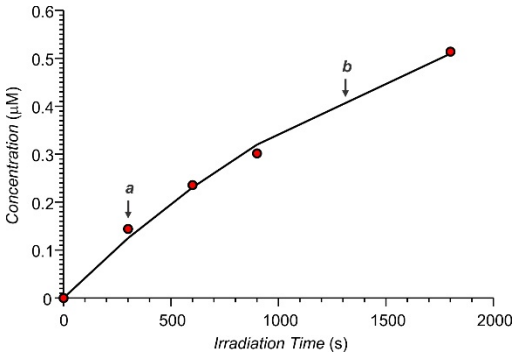

Figure S3. Plot (***a***) of the concentration of **2** against the irradiation time, extracted from the HPLC traces in Figure S2, with the corresponding fitting (***b***) to equation (4).

Table S1. Absorption (λ_{Ab}) and emission (λ_{Em}) wavelengths, molar absorption coefficient (ε), fluorescence quantum yield (ϕ_F), brightness ($\varepsilon \times \phi_F$) and activation quantum yield (ϕ_A) of **1**–**3** in aerated MeCN at 25 °C [*a*].

	λ_{Ab} (nm)	λ_{Em} (nm)	ε ($mM^{-1}\ cm^{-1}$)	ϕ_F (10^{-2})	$\varepsilon \times \phi_F$ ($mM^{-1}\ cm^{-1}$)	ϕ_A (10^{-3})
1	574	587	95.1	1	1	1
2	619	628	69.5	4	3	3
3	663	673	84.5	16	14	—

[*a*] The values of ϕ_F were determined against EtOH solutions of either the acetate salt of Cresyl Violet (ϕ_F = 0.54) or the perchlorate salt of Oxazine 1 (ϕ_F = 0.15). The values of ϕ_A were determined against a potassium ferrioxalate actinometer from the temporal evolution of the concentration of **2** during photolysis (Figure S2).

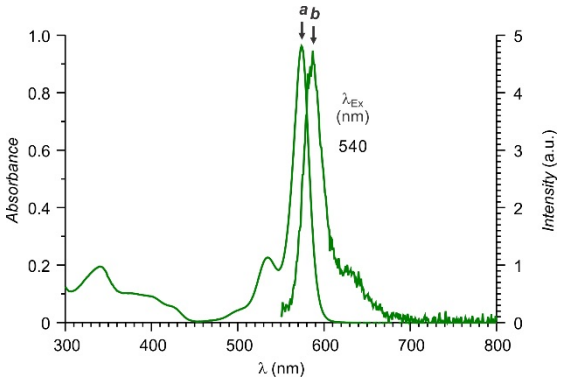

Figure S4. Absorption (***a***) and emission (***b***) spectra of **1** (10 μM) in MeCN at 25 °C.

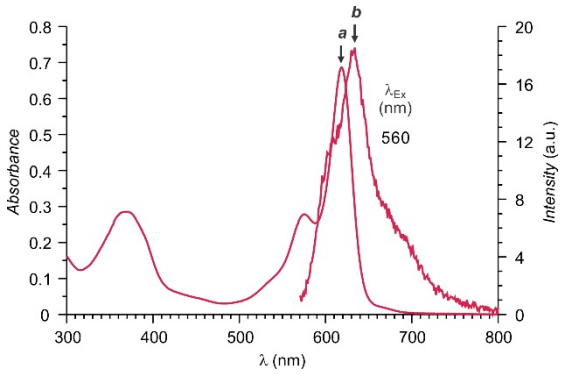

Figure S5. Absorption (***a***) and emission (***b***) spectra of **2** (10 μM) in MeCN at 25 °C.

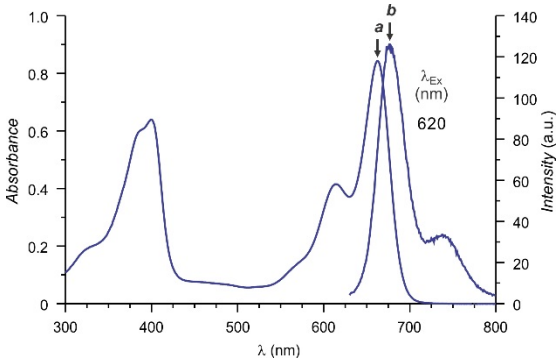

Figure S6. Absorption (***a***) and emission (***b***) spectra of **3** (10 μM) in MeCN at 25 °C.

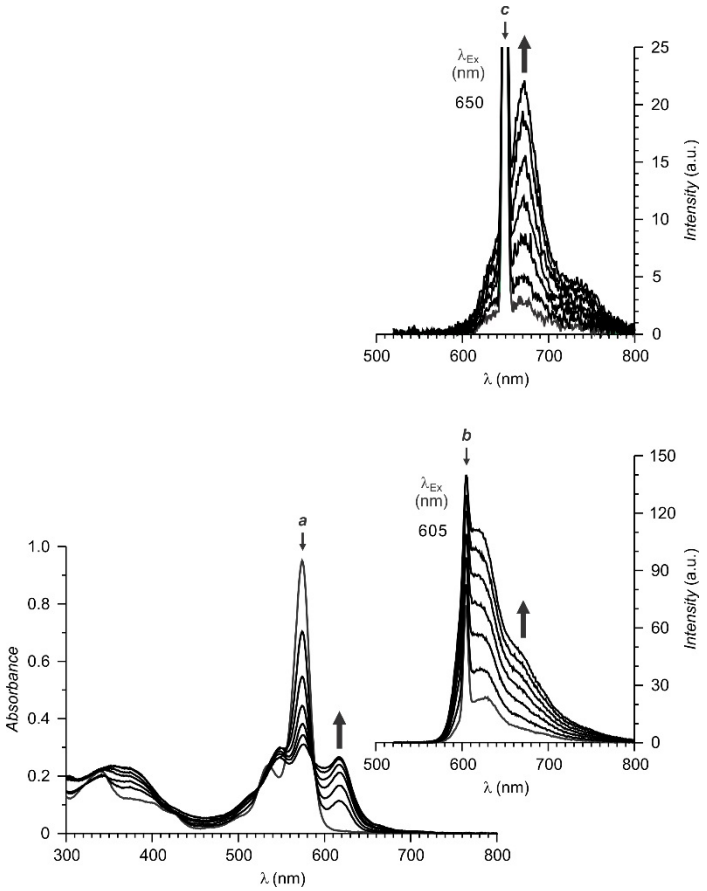

Figure S7. Absorption (***a***) and emission (***b*** and ***c***) spectra recorded before and during the photolysis (λ_{Ac} = 350 nm, 4.2 mW cm^{-2}) of a MeCN solution of **1** (10 μM) for 30 min at 25 °C.

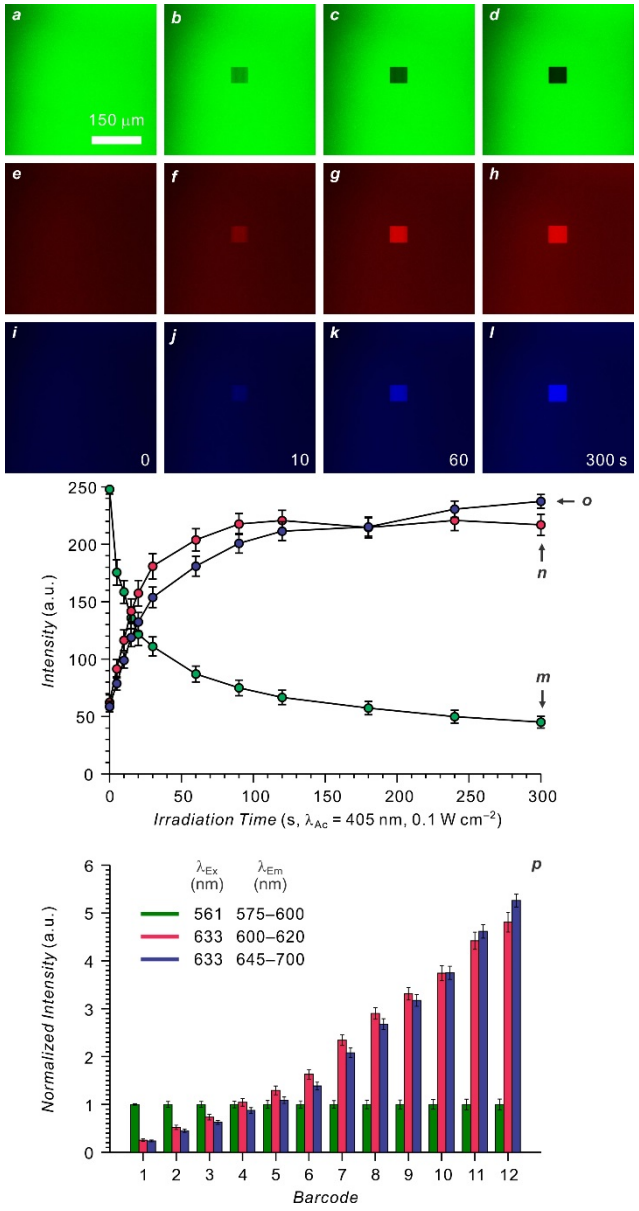

Figure S8. Fluorescence images of a PMMA film, doped with **1** (0.25% w/w), before (***a***, ***e*** and ***i***) and after (***b***–***d***, ***f***–***h*** and ***j***–***l***) irradiation of a square in the center of the imaging field for increasing times, temporal evolutions of the average emission intensities (***m***–***o***), measured in the central square, and corresponding relative emission intensities (***p***).

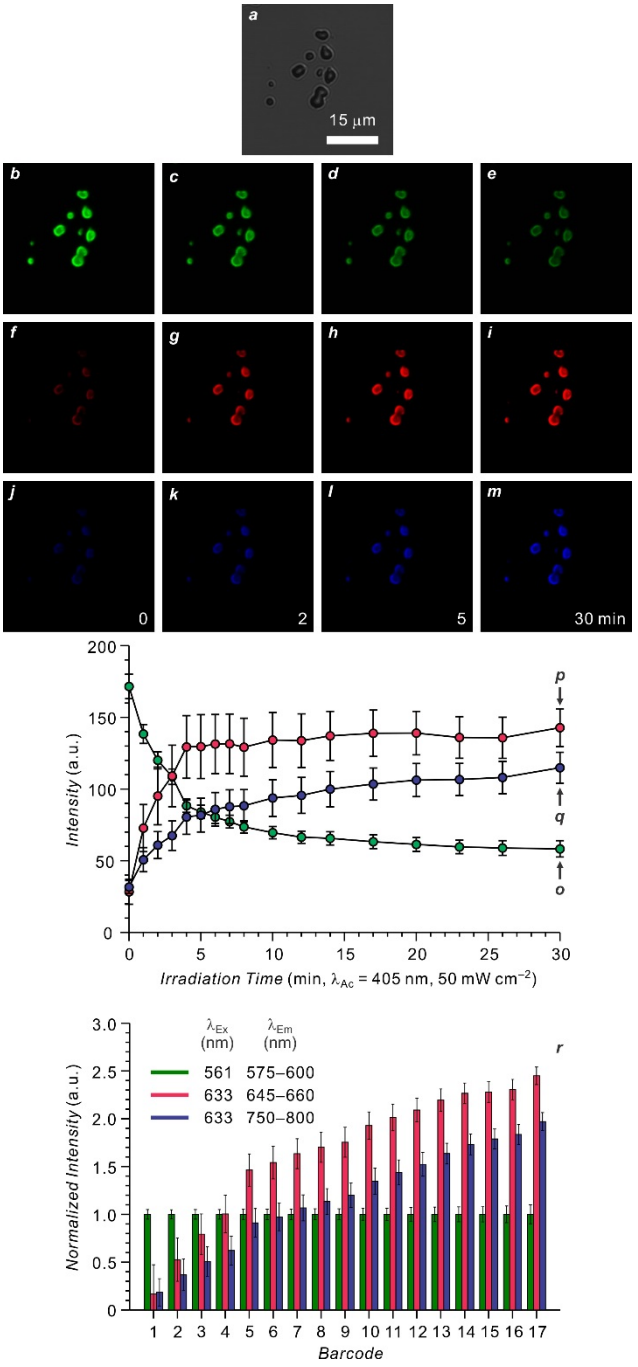

Figure S9. Brightfield (***a***) and fluorescence images of PS beads, doped with **1** (5% w/w), recorded before (***b***, ***f*** and ***j***) and after (***c***–***e***, ***g***–***i*** and ***k***–***m***) irradiation of the entire imaging field for increasing times, temporal evolutions of the emission intensities (***o***–***q***), averaged across five beads, and corresponding relative emission intensities (***r***).

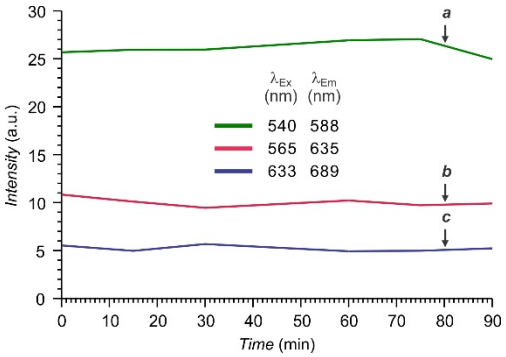

Figure S10. Temporal dependence of the emission intensities of PS beads, doped with **1** (***a***), **2** (***b***) and **3** (***c***), in H_2O at 25 °C.

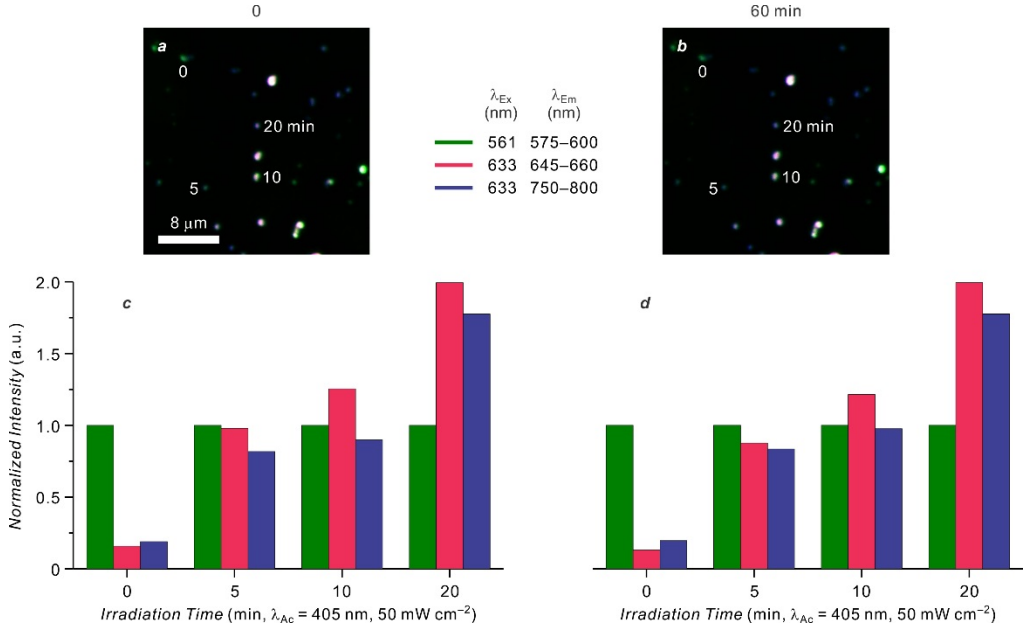

Figure S11. Overlaps of three fluorescence channels (***a*** and ***b***) and corresponding relative emission intensities (***c*** and **d**) of PS beads, doped with **1** (5% w/w), recorded after irradiation of individual beads for different times before (***a*** and ***c***) and after (***b*** and ***d***) storage for 60 min.

Web Enanched Object

Video S1. Sequence of fluorescence images (456 × 489 μm^2, λ_{Ex} = 561 nm, λ_{Em} = 575–600 nm) of a *C. elegans* labeled with PS beads, doped with **1** (5% w/w), recorded with a frame time of 470 ms.

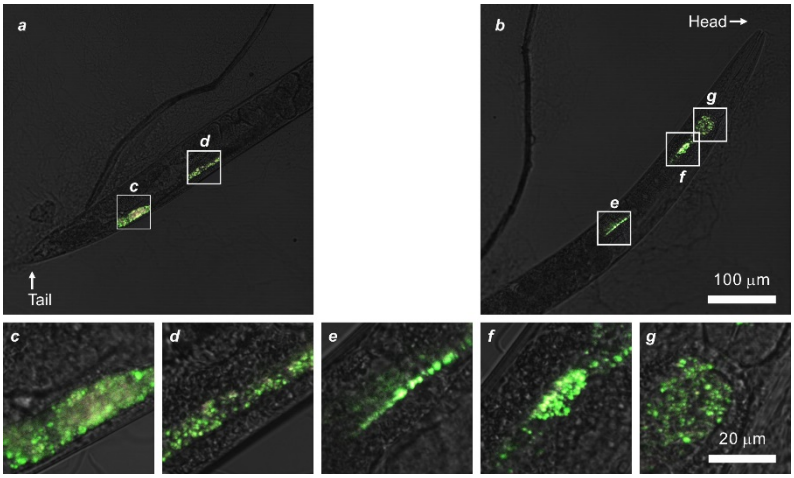

Figure S12. Overlaps (***a*** and ***b***) of brightfield images and three fluorescence channels (green: λ_{Ex} = 561 nm, λ_{Em} = 575–600 nm; red: λ_{Ex} = 633 nm, λ_{Em} = 645–660 nm; blue: λ_{Ex} = 633 nm, λ_{Em} = 750–800 nm) of a *C. elegans* labeled with PS beads, doped with **1** (5% w/w), and magnifications (***c***–***g***) of selected regions.

Web Enanched Object

Video S2. Sequence of fluorescence images (194 × 194 μm^2, λ_{Ex} = 561 nm, λ_{Em} = 575–600 nm) of a *C. elegans* labeled with PS beads, doped with **1** (5% w/w), recorded with a frame time of 567 ms after illumination (λ_{Ac} = 405 nm, 50 mW cm^{-2}) of two distinct regions within the nematode for 5 and 10 min respectively and storage for 50 min.